

Contents lists available at ScienceDirect

Quaternary Science Reviews

journal homepage: www.elsevier.com/locate/quascirev



The spatio-temporal pattern of Asian summer monsoon during glacial Termination II recorded by Chinese stalagmite δ^{18} O



Wei Jia ^{a, b, c}, Pingzhong Zhang ^{a, *}, Xianfeng Wang ^{b, c}, Shaoneng He ^b, Guangxin Liu ^d, Hongyu Shi ^a, Binggui Cai ^{e, f}, Shufang Yuan ^{b, c}, Wenfei Zhang ^a, Ruitao Deng ^a, Leilei Zhang ^a, Tao Gao ^a, Qibin Sun ^{g, h}, Hai Cheng ⁱ, Youfeng Ning ⁱ, R. Lawrence Edwards ^j

- a Key Laboratory of Mineral Resources in Western China (Gansu Province), School of Earth Sciences, Lanzhou University, Lanzhou, 730000, China
- ^b Earth Observatory of Singapore, Nanyang Technological University, Singapore, 639798, Singapore
- ^c Asian School of the Environment, Nanyang Technological University, Singapore, 639798, Singapore
- ^d Department of Atmospheric Science, Yunnan University, Kunming, 650500, China
- e Key Laboratory for Humid Subtropical Eco-Geographical Processes of the Ministry of Education, Fujian Normal University, Fuzhou, 350007, China
- f Institute of Geography, Fujian Normal University, Fuzhou, 350007, China
- g School of Atmospheric Sciences, Guangdong Province Key Laboratory for Climate Change and Natural Disaster Studies, Sun Yat-sen University, Guangdong, 519082. China
- $^{
 m h}$ Institute of Earth Climate and Environment System, Sun Yat-sen University, Guangdong, 519082, China
- ⁱ Institute of Global Environmental Change, Xi'an Jiaotong University, Xi'an, 710054, China
- ^j Department of Environmental and Earth Sciences, University of Minnesota, Minneapolis, MN, 55455, USA

ARTICLE INFO

Article history: Received 17 January 2023 Received in revised form 12 June 2023 Accepted 12 June 2023 Available online 23 June 2023

Handling Editor: Mira Matthews

Keywords:
Wanxiang cave δ¹⁸O
Western China
Asian summer monsoon
Westerly jet
Moisture source
Glacial termination II

ABSTRACT

The difficulty in constraining the large-scale Asian summer monsoon (ASM) variability in the Chinese monsoon region (CMR) during glacial Termination II lies in our limited knowledge of the western part, primarily due to sparse paleoclimate records. To get a better picture of the ASM during Termination II, we examined a precisely dated stalagmite δ^{18} O record between 133.1 and 127.0 kyr B.P. from Wanxiang Cave located at the ASM's northern edge in western China. In combination with published δ^{18} O data from this cave, we have identified the 'Weak Monsoon Interval' (WMI) in the Wanxiang δ^{18} O record and confirmed that the Heinrich 11 cold event in the North Atlantic caused the weakened ASM over the CMR via reorganization of the large-scale ocean-atmospheric circulation. However, the post-WMI change in δ^{18} O is gradual, in contrast with the abrupt shift shown in the other cave records from southern and northeastern China. The rapid northward migration of the westerly jet relative to the Qinghai-Tibet Plateau is probably responsible for this discrepancy. This northward-positioned westerly jet prevented the more ¹⁸O-depleted moisture from the Indian Ocean from reaching the study site. Simultaneously, it facilitated the earlier northward movement of the East Asian summer monsoon (EASM) rainband that carries positive precipitation δ^{18} O to obscure the abrupt decrease in our δ^{18} O record. After the onset of the last interglacial, no obvious Younger Dryas (YD)-like event was recorded in Wanxiang Cave. This result is consistent with most stalagmite δ^{18} O records in the CMR and further suggests a minimal impact of the YD-like event on ASM variabilities. The relatively large amplitude of δ^{18} O variations observed in Wanxiang Cave between the late penultimate glacial and the last interglacial corresponds to a dominant control of the Indian summer monsoon (ISM), whereas smaller δ^{18} O amplitudes were recorded in cave sites mainly under the influence of both ISM and EASM. Therefore, we posit that the heterogeneity of the hydroclimate in the CMR during Termination II resulted from a combination of multiple processes, that is, the westerly jet, ISM and EASM, rather than a single one.

© 2023 The Authors. Published by Elsevier Ltd. This is an open access article under the CC BY-NC-ND license (http://creativecommons.org/licenses/by-nc-nd/4.0/).

1. Introduction

Knowledge of the regulations and driving mechanisms of glacial and interglacial climatic cycles is critical for understanding

^{*} Corresponding author. E-mail address: pzzhang@lzu.edu.cn (P. Zhang).

potential abrupt climate changes under continuous global warming. The glacial 'Termination II', i.e., the penultimate deglaciation, experienced an abrupt climate shift during the transition from a full glacial state to an interglacial state, accompanied by a considerable rise in sea level (Siddall et al., 2006; Denton et al., 2010; Grant et al., 2012) and an increase in atmospheric CO₂ (Lourantou et al., 2010). Various paleoclimate archives have been used to uncover this climate transition, namely pollen (Sánchez Goñi et al., 1999), stalagmites (Drysdale et al., 2009; Moseley et al., 2015; Magiera et al., 2019; Stoll et al., 2022), tufa (Domínguez-Villar et al., 2020), and deep-sea sediments (Deaney et al., 2017). Among them, the stalagmite $\delta^{18}\text{O}$ records from the Chinese monsoon region (CMR) reveal a tight linkage between the Asian summer monsoon (ASM) and the climate conditions over the high latitudes during Termination II (e.g., Cheng et al., 2006, 2009; Wang et al., 2008; Cai et al., 2015; Duan et al., 2019; Xue et al., 2019; Wassenburg et al., 2021). For example, Heinrich stadial 11 (HS 11) cold period and the associated ice rafted debris (IRD) event originated in the North Atlantic and coincided with the 'Weak Monsoon Interval' (WMI) in China (e.g., Cheng et al., 2009; Duan et al., 2019). The bipolar seesaw hypothesis has been used to explain the ASM variations during Termination II (Kelly et al., 2006; Masson-Delmotte et al., 2010; Li et al., 2014). However, there are still some discrepancies among Chinese stalagmite δ^{18} O records regarding the identification of climate events on centennial to millennial timescales. For instance, Xue et al. (2019) reported a Younger Dryas-like (YD-like) event in their stalagmite record with an abrupt positive δ^{18} O shift (weakening ASM) between 128.5 and 128.1 kyr B.P. during Termination II from Shangxiaofeng Cave in northern China. Accordingly, they further suggested that this YD-like event should be considered as an intrinsic feature of climate change during ice age terminations. Other Chinese stalagmite δ^{18} O records, however, do not seem to capture any YD-like event (e.g., Kelly et al., 2006; Cheng et al., 2009; Li et al., 2014; Duan et al., 2019; Liu et al., 2020). In addition, a northern Chinese stalagmite δ^{18} O record from Xinglong Cave suggests that the short δ^{18} O excursion between 128.5 and 127.5 kyr B.P. probably does not represent a YD-like event because of its much smaller magnitude relative to the actual YD event during Termination I (Duan et al., 2019). Alternatively, there was a 'pause' in the stalagmite δ^{18} O records in northern China, synchronous with a 'slowdown' phase during the $\delta^{18}O$ decrease in cave records from southern China (Duan et al., 2019). It is noteworthy that this northsouth contrast in stalagmite $\delta^{18}O$ was only based on a limited number of δ^{18} O records from eastern and southern China. More stalagmite records from widespread locations in the CMR are needed to confirm these specific events.

Multiple mechanisms have been proposed to elucidate the discrepancies among the Chinese stalagmite δ^{18} O records during the penultimate deglaciation, such as differences in altitude (Cai et al., 2012) and moisture source (Cai et al., 2015), sea level changes (Xue et al., 2019), and the transport pathway effect (Liu et al., 2020). But it remains unclear which of these mechanisms were dominant. Besides, the evolution of the ASM in western China close to the modern summer monsoon boundary during the penultimate deglaciation remains enigmatic, as published stalagmite records of the CMR are mostly from southern and northern China. Therefore, it is vital to explore the underlying mechanisms of the ASM variabilities by investigating stalagmite records from other sites in the CMR.

Located near the margin of modern summer monsoon, western China lies in the interaction zone of mid-latitude westerly jet, and the East Asian summer monsoon (EASM) and Indian summer monsoon (ISM) from the low latitudes. This region is sensitive to precipitation change caused by the meridional movement of the ASM. As such, monsoonal precipitation variations in this region are

a reliable indicator of ASM strength (Johnson et al., 2006; Zhang et al., 2008). When the circulation associated with the ASM is intensified (weakened), more (less) water vapor from the western Pacific and/or the tropical Indian Ocean is carried into western China, leading to higher (lower) regional precipitation (Tan, 2014; Hu et al., 2019; Jia et al., 2022a). Paleoclimate archives from western China thus have the potential to provide a new perspective on the ASM variabilities in the CMR. In this study, we present a precisely dated and high-resolution stalagmite stable isotope record collected from Wanxiang Cave in western China, spanning the penultimate deglaciation period (from 133.1 to 127.0 kyr B.P.). We aim to characterize the regional variation of precipitation $\delta^{18}O$ and its linkage to the ASM in western China. Additionally, we combined our record with other stalagmite records from different sites in the CMR to explore the spatial distribution of millennial-scale climate events and their dynamic linkages. Our investigation enhances our understanding of how changes in the ASM affect the hydroclimatic responses in the study region.

2. Material and methods

2.1. Cave site and regional climate

Wanxiang Cave (33°19′N, 105°00′E, 1200 m a. s. l.) is located in the transition zone between the western Loess Plateau and the eastern Qinghai-Tibet Plateau, Gansu Province in western China. This area is near to the marginal zone under the influence of the modern summer monsoon and thus its precipitation records the ASM evolution (Fig. 1). Lying in the climate transitional zone between the north subtropics and temperate zone, Wanxiang Cave site is characterized by warm/wet summer and cold/dry winter with a mean annual temperature of 12 °C and a mean annual precipitation of 460 mm, 80% of which occurs during the summer monsoon season between May and September (Johnson et al., 2006; Zhang et al., 2008).

The cave has a small entrance but with a large complex karst system. Field observations show that the cave is weakly ventilated, experiencing constant temperature of ~11 °C and relative humidity of 95%—100% throughout the year (Zhang et al., 2004). The cave is developed in Carboniferous limestone, overlain by 30—250 m thick bedrock and ~10 m of loess with dense vegetation. The local vegetation is dominated by C3 plants (i.e., *Chrysanthemum, Artemisia*) with a small abundance of C4 plants (*Arrowbamboo and Gramineae*) (Jia et al., 2022b).

2.2. Sampling

Stalagmite WXZ05-12, with a total length of 382 mm and a diameter of ~115 mm, was collected ~1200 m away from the cave entrance and ~12 m below the roof. The stalagmite has a 'candle-stick' shape, suggesting a fairly stable growth history. The specimen was halved along the growth axis by using a diamond saw and then polished. The polished surface shows gray to brownish colors (Fig. S1). Also, the specimen is highly crystalized with dense lamination, indicating a continuous deposition. Sub-samples for chemical analysis, including 6 for ²³⁰Th dating and 644 for oxygen and carbon stable isotope measurements, were collected along the growth axis of the stalagmite by using 0.5-mm-diameter carbide dental drill bits.

2.3. Isotope analyses

²³⁰Th dating were performed on a Thermo-Fisher NEPTUNE, a multi-collector inductively coupled plasma mass spectrometer (MC-ICP-MS) at the Isotope Laboratory, Xi'an Jiaotong University,

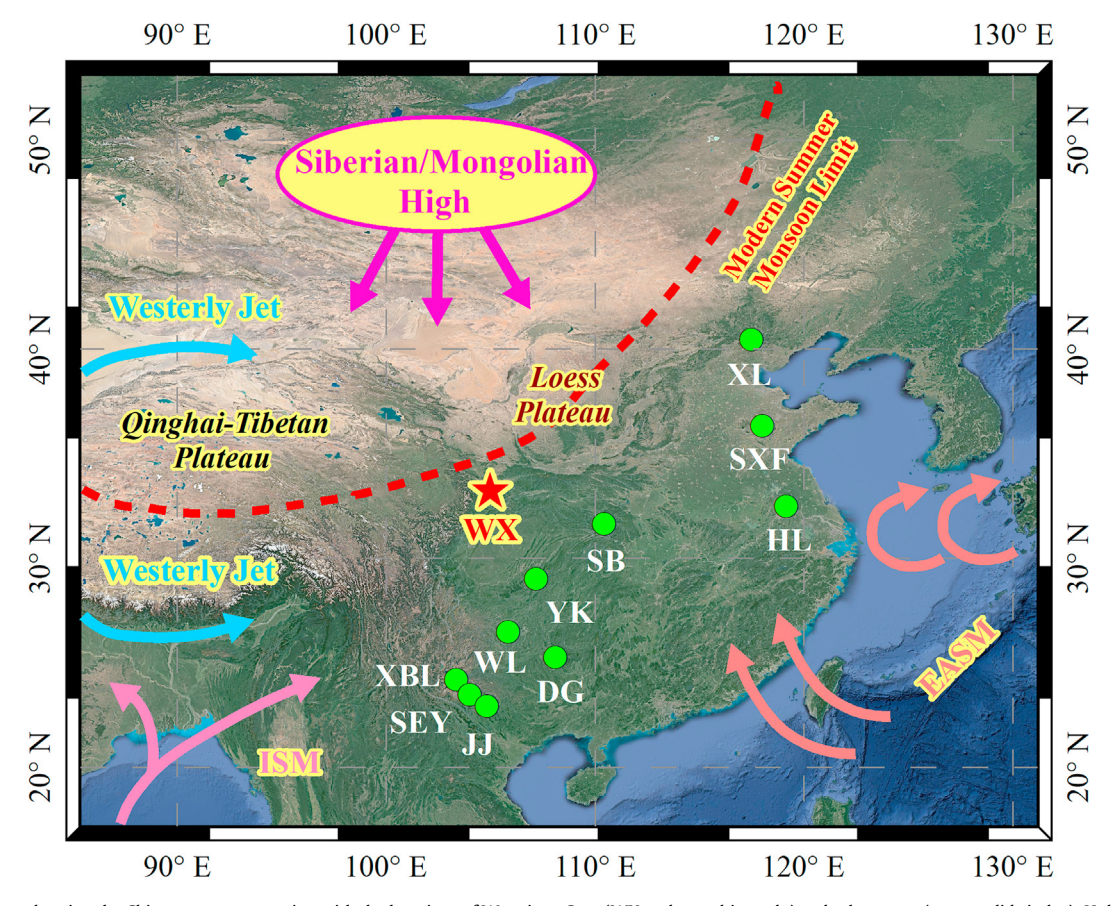


Fig. 1. Regional map showing the Chinese monsoon region with the locations of Wanxiang Cave (WX, red star, this study) and other caves (green solid circles): Hulu Cave (HL; Cheng et al., 2006), Sanbao Cave (SB; Wang et al., 2008; Cheng et al., 2009), Xinglong Cave (XL; Duan et al., 2019), Shangxiaofeng Cave (SXF; Xue et al., 2019), Yangkou Cave (YK; Li et al., 2014), Xiaobailong Cave (XBL; Cai et al., 2012), Wulu Cave (WL; Liu et al., 2022), Southeast Yunnan Cave (SEY; Liu et al., 2020), Jiangjun Cave (JJ; Wassenburg et al., 2021), and Dongge Cave (DG; Kelly et al., 2006). The red dashed line indicates the modern summer monsoon limit (modified by Zhang et al., 2008). The deep orange and light pink arrows represent the East Asian summer monsoon (EASM) and the Indian summer monsoon (ISM), respectively. The blue arrows indicate the mid-latitude westerly jet relative to the Qinghai-Tibetan Plateau.

China. We followed the chemical procedures by Edwards et al. (1987) to extract uranium and thorium, and the measuring protocol by Cheng et al. (2013).

Stable isotopes were analyzed on a Finnigan-MAT 253 plus mass spectrometer equipped with a Kiel-IV Carbonate Device at the School of Geographical Sciences, Fujian Normal University, China. The interlaboratory standard TTB1 was run every 10–20 samples. The results are reported as δ -values relative to Vienna PeeDee Belemnite (VPDB). Precision for $\delta^{18}\text{O}$ is better than 0.06‰ and $\delta^{13}\text{C}$ is better than 0.03‰, at the 1σ level.

3. Results

3.1. Chronology

High concentrations of uranium (4298.7–7201.9 ppb) and low concentrations of thorium (352–1387 ppt) facilitate the robustness of dating results. All the ^{230}Th dates are in a stratigraphic order within errors (2 σ) ranging from 310 to 425 yr (Table S1). We established the age model for stalagmite WXZ05-12 by using a linear interpolation between the ^{230}Th dates (Fig. S1). According to this age model, the WXZ05-12 grew continuously between 133.1 and 127.0 kyr B.P., a period that covers the latter portion of the penultimate glacial and the subsequent transition into the early part of last interglacial.

3.2. δ^{18} O record

The WXZ05-12 $\delta^{18}O$ shows a large variation, ranging from -5.32% to -11.58% (Fig. 2). The ramp function regression analysis (Mudelsee, 2000) identified four ramps with the second transition corresponding to a slight increase in $\delta^{18}O$, and the other three corresponding to a rapid decrease in $\delta^{18}O$. Overall, $\delta^{18}O$ exhibits a gradual decreasing trend on millennial timescales, interrupted by a small positive excursion between 129.8 and 129.4 kyr B.P. (Fig. 2).

3.3. Fidelity of δ^{18} O as a climate proxy

The Hendy's criterion (Hendy, 1971) was used to evaluate whether the WXZ05-12 $\delta^{18}O$ data can be used as paleoclimate indicators. We drilled 16 sub-samples along four horizontal layers and examined variations of $\delta^{18}O$ and $\delta^{13}C$ along each lamina. Nearly identical $\delta^{18}O$ values were found in individual layers and there is no significant correlation between $\delta^{18}O$ and $\delta^{13}C$ along the layers, which suggests that the calcite of stalagmite WXZ05-12 was deposited under nearly isotopic equilibrium conditions (Hendy, 1971) (Fig. S2). The replication test is another approach, probably more robust, to check the fidelity of speleothem isotope time series as a paleoclimate recorder (Cheng et al., 2006, 2009; Dorale and Liu, 2009). Like other Chinese stalagmite $\delta^{18}O$ records, the WXZ05-12

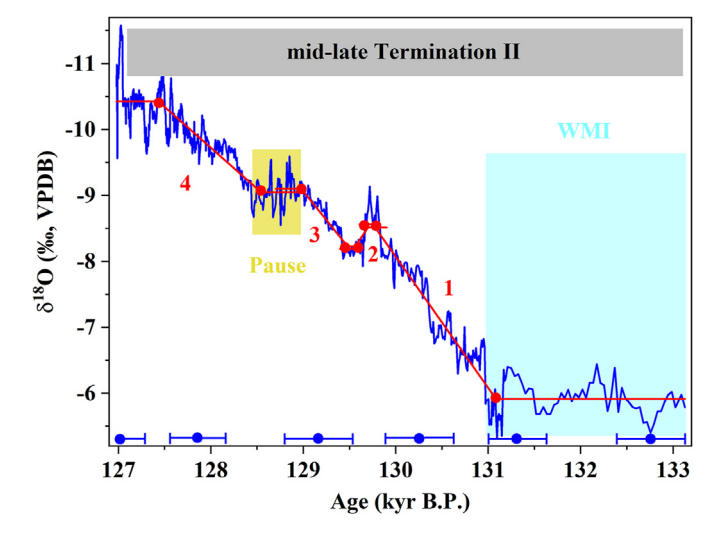


Fig. 2. Stalagmite WXZ05-12 δ^{18} O time series (deep blue line). The 230 Th dates with uncertainties ($\pm 2\sigma$) are shown below the δ^{18} O profile. The light blue bar indicates the 'Weak Monsoon Interval' (WMI) (Cheng et al., 2009). The deep yellow bar depicts the climate 'pause' after the onset of the last interglacial (Duan et al., 2019). The red lines show the four-fold ramp function that was fitted to WXZ05-12 δ^{18} O.

 δ^{18} O data also display a negative change during the same growth interval (Fig. 3). This similarity suggests that our δ^{18} O record primarily represents large-scale climatic signals. The δ^{18} O of stalagmite WXZ05-12, therefore, can be regarded as a robust proxy for paleoclimate change.

Stalagmite δ^{18} O is controlled by drip water δ^{18} O (Hendy, 1971) and cave temperature (McCrea, 1950). However, the temperaturedependent fractionation between the calcite and water is -0.23%/°C (Kim and O'Neil, 1997), while the mean annual atmospheric temperature in East Asia only increased by \sim 3.4 \pm 1.0 °C during Termination II (Duan et al., 2022). Besides, the TEX₈₆ temperature record established by the Jiangjun Cave stalagmites, southwestern China, showed an abrupt increase of ~4 °C after ~130 kyr B.P. (Wassenburg et al., 2021). Therefore, the primary control of the large change in WXZ05-12 δ^{18} O (~6.26%) should be the drip water δ^{18} O in the cave. δ^{18} O of drip water largely inherits that of meteoric precipitation, and thus records the variation in precipitation δ^{18} O related to ASM intensity (Zhang et al., 2004; Johnson et al., 2006). Although the interpretations of Chinese stalagmite δ^{18} O records remain somewhat controversial because of the possible influence from summer/winter precipitation ratio (Wang et al., 2001), cloud-top pressure (Cai et al., 2017), and the circulation effect (Tan, 2014), the stalagmite δ^{18} O records in the CMR nevertheless resemble Greenland ice core $\delta^{18}\text{O}$ records on millennial scales (e.g., Wang et al., 2001; Duan et al., 2019). Hence, the Chinese stalagmite δ^{18} O can be tied to summer precipitation δ¹⁸O associated with ASM intensity (e.g., Wang et al., 2008; Cheng et al., 2019; Xue et al., 2019; Jia et al., 2022a). Furthermore, both climate model simulations and synthesized Chinese stalagmite δ^{18} O records have confirmed that the millennial-scale δ^{18} O records reflect the ASM intensity with decreasing (increasing) δ¹⁸O corresponding to a strengthening (weakening) of the ASM intensity (e.g., Liu et al., 2014; Hu et al., 2019). In conclusion, the WXZ05-12 δ^{18} O record is interpreted as an indicator of precipitation variations associated with ASM intensity on millennial timescales. Following Cheng et al. (2006, 2019), we apply the terms 'low' and 'high' stalagmite δ^{18} O to represent 'strong ASM' and 'weak ASM' accompanying with 'increased' and 'decreased' regional precipitation amount, respectively.

4 Discussion

4.1. The 'WMI' event during Termination II

Stalagmite δ^{18} O records from southern and northern Chinese caves reveal a WMI event with relatively high δ^{18} O values prior to the onset of the last interglacial, i.e., a weakened ASM, corresponding to HS 11 (cold event) in the North Atlantic (e.g., Cheng et al., 2006; Duan et al., 2019). To trace the presence of the WMI in western China, we combined stalagmite $\hat{\delta}^{18}$ O data from Wanxiang Cave (WXSM 51 and WXSM 52, Johnson et al., 2006; WXB075, Gao et al., 2023) with the WXZ05-12 δ^{18} O, and compared them with other Chinese stalagmite $\delta^{18}O$ between 150 and 123 kyr B.P. (Fig. 3). Although the WXZ05-12 δ^{18} O record does not overlap the WXB075, WXSM51, and WXSM52 records, these three stalagmites grew near our stalagmite WXZ0510. This indicates that they were likely deposited under similar growth conditions, including seepage channels and roof permeability. In addition, the WXSM51 δ^{18} O record (Johnson et al., 2006) partly overlaps the WXB075 δ^{18} O data (Gao et al., 2023) between ~125 and ~126 kyr B.P. Therefore, our splicing records are robust considering large-scale variations in δ^{18} O from 150 to 123 kyr B.P. (Fig. 3A). A broad agreement between the splicing δ^{18} O records (δ^{18} O_s; Fig. 3A) and other cave $\delta^{18}O$ records in the CMR further confirms the consistent millennial-scale evolution of the ASM on a continental scale. Most importantly, the $\delta^{18}O_s$ record captures the WMI approximately from 141.2 to 130.2 kyr B.P. defined by Cheng et al. (2006, 2009), which consists of an intensively abrupt positive shift in δ^{18} O at its inception and an abrupt negative shift in δ^{18} O near its end. This suggests that HS 11 has indeed led to a large-scale weakening of ASM intensity across the CMR. The gradual increase in Northern Hemisphere summer insolation (NHSI) (65°N) (Berger, 1978) triggered the initial retreat of northern hemisphere ice sheets (Fig. 4I) and thus resulted in major meltwater pulses into the North Atlantic (Fig. 4A) (HS 11; Skinner and Shackleton, 2006; Mokeddem et al., 2014). The influx of freshwater, in turn, induced a shut-down of the Atlantic Meridional Overturning Circulation (AMOC) (Fig. 4B; Deaney et al., 2017) with lower sea surface temperature (SST) in the North Atlantic (Fig. 4D; Skinner and Shackleton, 2006; Tzedakis et al., 2018), largely reducing the surface-ocean heat transport to the North Atlantic (Cheng et al., 2006). Simultaneously, a gradual increase in the Antarctic temperature (Fig. 4G; Jouzel et al., 2007) weakened the Somali jet, the Mascarene High, and northward cross-equatorial airflows (Tiwari et al., 2021). With an accumulation of more latent heat and moisture in the Southern Hemisphere (Fig. 4F; Shackleton et al., 2020), the southward positioned Intertropical Convergence Zone (ITCZ) (Fig. 4E; Gibson and Peterson, 2014) and the collapsed AMOC could not provide a strong impetus for the ASM, leading to less monsoonal precipitation over the CMR (lia et al., 2022a).

It is worth noting that the duration of the WMI recorded by the Wanxiang Cave (Fig. 3A), Southeast Yunnan Cave (Fig. 3B), Wulu Cave (Fig. 3C), Jiangjun Cave (Fig. 3D), and Xiaobailong Cave (Fig. 3E) δ^{18} O records appears longer than that captured by other cave δ^{18} O records (Fig. 3F–K). According to the criterion set by Cheng et al. (2006, 2009), the WMI event lasts ~11 kyr in Wanxiang Cave, ~11.2 kyr in Southeast Yunnan Cave, ~12.2 kyr in Wulu Cave, and ~9.2 kyr in Jiangjun Cave, respectively. Albeit its relatively lower resolution (Fig. 3E; Cai et al., 2015), the Xiaobailong Cave δ^{18} O record presents one-to-one correlation with the higher-resolution Sanbao Cave δ^{18} O records (Cheng et al., 2006, 2009), and thus we determine ~12.8 kyr as the duration of the WMI in Xiaobailong Cave (Cai et al., 2015). However, other cave δ^{18} O records, i.e., Yangkou Cave, Dongge Cave, Sanbao Cave, Hulu Cave, Shangxiaofeng Cave, and Xinglong Cave, have a shorter WMI with less than ~8 kyr

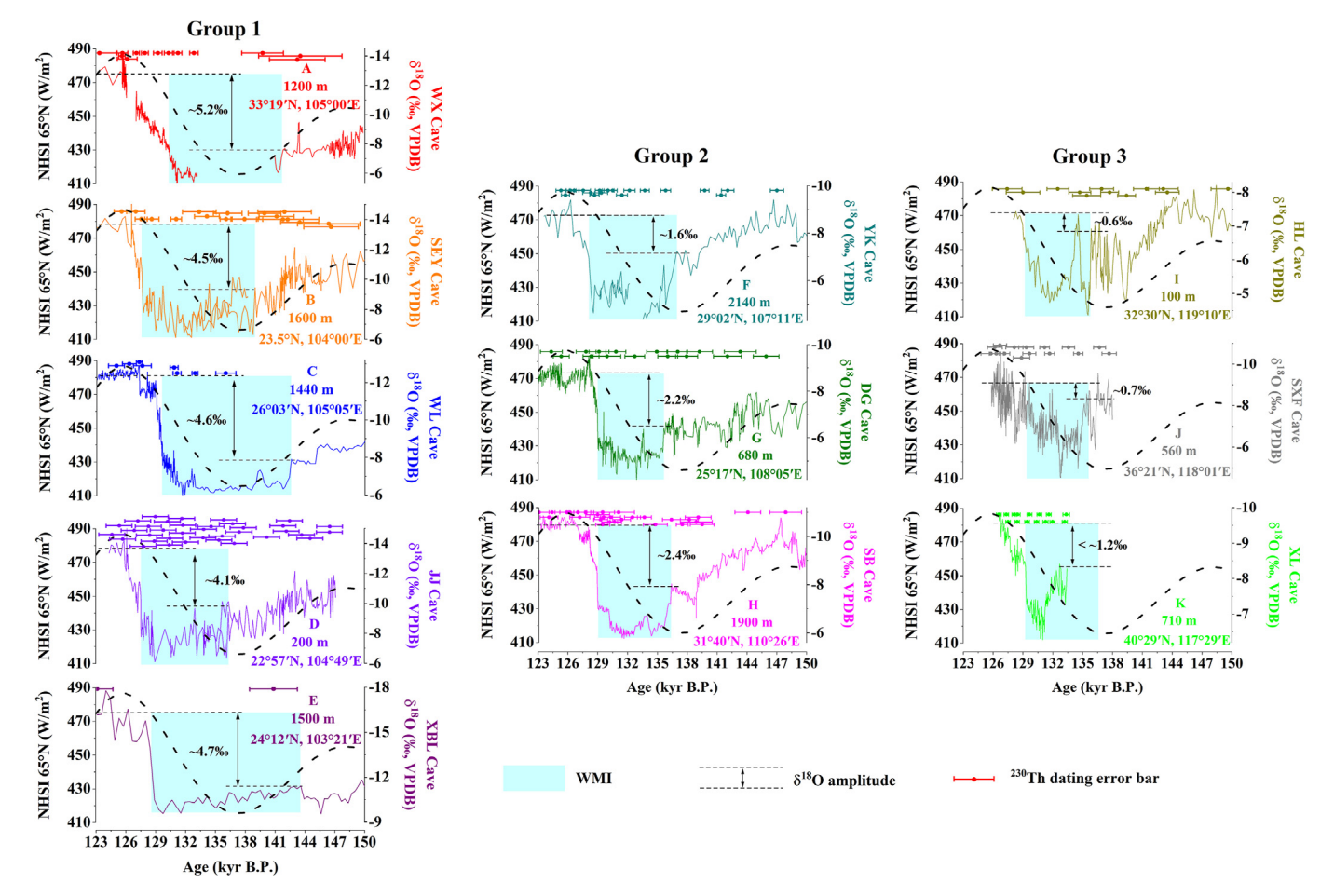


Fig. 3. A comparison of stalagmite δ^{18} O records in the Chinese monsoon region. The δ^{18} O records in 'Group 1' that are mainly influenced by the ISM includes: (A) Wanxiang Cave (WX; this study), (B) Southeast Yunnan Cave (SEY; Liu et al., 2020), (C) Wulu Cave (WL; Li et al., 2022), (D) Jiangjun Cave (JJ; Wassenburg et al., 2021), and (E) Xiaobailong Cave (XBL; Cai et al., 2015). The (F) Yangkou Cave (YK; Li et al., 2014), (G) Dongge Cave (DG; Kelly et al., 2006), and (H) Sanbao Cave (SB; Cheng et al., 2009) δ^{18} O records in 'Group 2' are possibly modulated by the ISM and EASM. The EASM largely controls those δ^{18} O records of (I) Hulu Cave (HL; Cheng et al., 2006), (J) Shangxiaofeng Cave (SXF; Xue et al., 2019), and (K) Xinglong Cave (XL; Duan et al., 2019) in 'Group 3'. The light blue bars indicate the 'WMI' event (Cheng et al., 2006, 2009). The black dashed lines depict the δ^{18} O amplitude based on the difference between each δ^{18} O of the last interglacial period and that of the period with an abrupt δ^{18} O shift right before HS 11 (Xue et al., 2019). The mean insolation in June, July and August at 65°N (NHSI 65°N) (Berger, 1978) is indicated by the black dashed curves. The information on altitude, latitude and longitude, and δ^{20} Th dates with uncertainties (δ^{20} C) are displayed on the right side and on the top of each plot, respectively.

(Fig. 3F–K). Although the Xinglong Cave $\delta^{18}O$ only partially covers the WMI, given its similar structure to the Hulu and Sanbao $\delta^{18}O$ records suggested by Duan et al. (2019), we suspect that they all have a comparable WMI duration (~7 kyr) (Fig. 3K). To date, it remains unclear what mechanisms caused the different durations of the WMI in the CMR. But since all the stalagmite $\delta^{18}O$ records registered the last interglacial onset at 129–130 kyr B.P. and they also responded rapidly to the HS 11 initiation, the longer WMI duration captured by the former five cave records could be attributed to their relatively low $\delta^{18}O$ resolution and/or uncertainties of the age control (Fig. 3A–E). Nevertheless, more high-resolution and precisely dated stalagmite records and model simulations are needed to validate the observed difference in the duration of the WMI.

4.2. The role of the westerly jet for $\delta^{18}\text{O}$ changes at the onset of the last interglacial

After the WMI, the sudden intensification of the ASM with a rapid negative δ^{18} O shift in a short period points to the onset of the last interglacial in the CMR (e.g., Kelly et al., 2006; Cheng et al., 2009; Li et al., 2014; Cai et al., 2015; Duan et al., 2019;

Wassenburg et al., 2021). This shift was accompanied by a rapid increase in the North Atlantic SST and atmospheric CH₄ in response to an abrupt reinforcement of the AMOC (Loulergue et al., 2008), manifesting a close teleconnection between the ASM and highlatitude climates (Fig. 4H) (Cheng et al., 2019; Jia et al., 2022a). Such a tipping point in the northern high latitudes, synchronous with the abrupt enhancement of the ASM, reflects the significant role of the bipolar seesaw mechanism in the abrupt climate shift (Kelly et al., 2006; Marino et al., 2015), However, the WXZ05-12 record exhibits a gradual negative change in δ^{18} O after the WMI rather than a rapid shift as recorded by most other Chinese stalagmite δ^{18} O records (Fig. 3). Likely, other factors may have prevented the swift recovery of the ASM signal from being transmitted to Wanxiang Cave site. The abrupt climate transition in the North Atlantic may not have had a profound influence on WXZ05-12 δ^{18} O at the last interglacial onset. Interestingly, this gradual variation in δ¹⁸O also seems to occur in Shangxiaofeng Cave, northern China (Fig. 3]). Thus, such attenuated ¹⁸O-depletion in both Wanxiang and Shangxiaofeng records might be influenced by a climate forcing other than the ASM changes.

The alteration of NHSI 65°N has been suggested as a major external driver of ASM fluctuations between glacial and interglacial

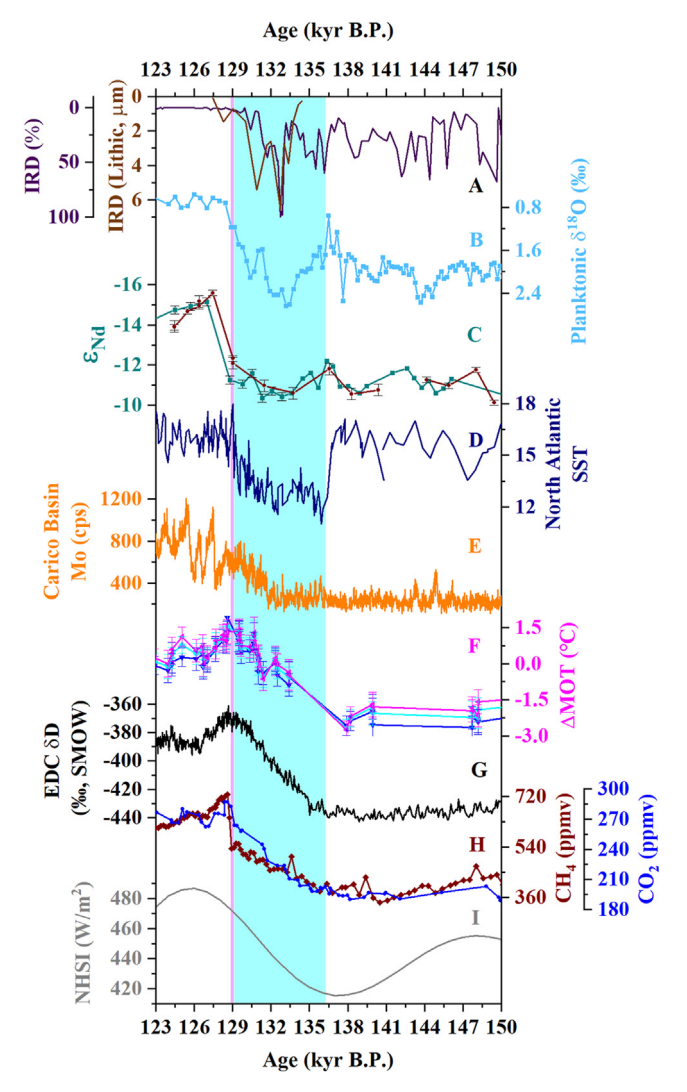


Fig. 4. Climate conditions at high-low latitudes between the late penultimate deglaciation and the last interglacial. (A) IRD record from sediment core MD01-2444 (deep yellow line; Skinner and Shackleton, 2006) digitized by Marino et al. (2015); IRD record from ODP site 984 (burgundy line; Mokeddem et al., 2014); (B) Planktic foraminiferal δ^{18} O from ODP Site 1063 (Deaney et al., 2017); (C) ϵ_{Nd} index from Bermuda Rise (Böhm et al., 2015); (D) North Atlantic sea surface temperature (Skinner and Shackleton, 2006; Tzedakis et al., 2018); (E) Mo element content record from the Cariaco basin (Gibson and Peterson, 2014); (F) Mean ocean temperature (Shackleton et al., 2020); (G) EDC ice core δD (Jouzel et al., 2007); (H) EDC ice core CO2 (deep blue line; Lourantou et al., 2010) and CH₄ concentration (brown line; Loulergue et al., 2008); (I) Mean insolation in June, July and August at 65°N (NHSI 65°N) (Berger, 1978). Duration of HS 11 is indicated by vertical cyan bar (Tzedakis et al., 2018). The purple line indicates the onset of the last interglacial at around 129 kyr B.P.

periods (e.g., Wang et al., 2001; Cheng et al., 2009). Due to its higher latitude position, the gradual negative variations in Wanxiang Cave $\delta^{18}\text{O}$ record might be influenced by the gradual increases in NHSI 65°N. However, the intensity of NHSI 65°N during the deglacial period was the same across the entire CMR, and the timing of the minimum $\delta^{18}\text{O}$ in all stalagmite records closely corresponded to the peak summer insolation intensity around 126–127 kyr B.P. within dating errors (Fig. 3). This implies minimal latitude and time lag effects of NHSI on Chinese stalagmite records in the CMR. Therefore, NHSI cannot explain the gradual changes in $\delta^{18}\text{O}$ observed in Wanxiang Cave.

A recent notion holds that the seasonal migration of the midlatitude westerly jet across the Qinghai-Tibet Plateau may be responsible for East Asian paleoclimate changes and ASM variability (Zhang et al., 2018; Li et al., 2019; Chiang et al., 2020; He et al., 2021; Jia et al., 2022a). There is also a close correlation between the Chinese stalagmite $\delta^{18}O$ and the aeolian dust abundance in central and eastern Asia; an increase (a decrease) in ASM intensity corresponds to a weak (a strong) westerly jet with its axis northward (southward) shift relative to the Oinghai-Tibetan Plateau during the last glacial period (Nagashima et al., 2007. 2011). Climate models also suggest that in boreal summer, the jet shifts north of the Qinghai-Tibetan Plateau (between 30°N and 40°N), with enhanced low-level (at about 850 hPa) southerly wind (Chiang et al., 2015; He et al., 2021; Liu et al., 2022). Besides, the westerly jet path varies in harmony with cold and warm events (Dansgaard-Oeschger cycles, HS) in the northern high-latitudes (Nagashima et al., 2011; Zhang et al., 2018; Li et al., 2019). Rapid shift from a cold (warm) period to a warm (cold) period in the high latitudes strengthened (decreased) the ASM, accompanied by a weak (strong) jet with a sudden northward (southward) shift relative to the Qinghai-Tibetan Plateau (Schiemann et al., 2009; Nagashima et al., 2011; Chiang et al., 2015; Kong et al., 2017). Modern observations demonstrate (e.g., Sato, 2009; Lei et al., 2021) that the westerly jet is also weak and located north of the Qinghai-Tibetan Plateau during the summer. However, the jet becomes enhanced and bifurcates in the winter, with a much stronger branch located south of the plateau and a much weaker one in the

At the onset of the last interglacial, a resumed AMOC (Fig. 4B: Deaney et al., 2017) and strengthened North Atlantic deep water (NADW) formation induced increasing northward latent heat transport (Fig. 4C; Böhm et al., 2015), and triggered a northward displacement of the ITCZ (Fig. 4E; Gibson and Peterson, 2014). The ITCZ drove the convection of the ascending branch of the Hadley circulation, resulting in an abrupt enhancement of the ASM (Jia et al., 2022a). Concurrently, an increase in the NHSI in the boreal summer reduced the pole-to-equator temperature gradient. This decreased temperature gradient led to a rapid northward shift of the westerly jet that remained at a southern location relative to the Qinghai-Tibetan Plateau during the HS 11 (Fig. 5A) (Kong et al., 2017; He et al., 2021; Lei et al., 2021). With this northward jet displacement, the ASM penetrated the interior of the CMR with a northward migration of the moisture flux (Fig. 5B) (Schiemann et al., 2009; Liu et al., 2014; Li et al., 2019; He et al., 2021). The caves in southern China, which been suppressed by the southern westerly jet during HS 11 (Li et al., 2022) (Fig. 5A), received large amounts of ASM precipitation during a short time period and thus displayed a rapid negative shift in stalagmite δ^{18} O. Moreover, a northward movement of the westerly jet controls the EASM seasonality with a significantly shorter Meiyu and a longer midsummer stage (Chiang et al., 2017; Kong et al., 2017; Zhang et al., 2018). A longer midsummer allows the monsoonal southerlies to penetrate northeastern China deeper (Liu et al., 2014; Orland et al., 2015; Zhang et al., 2018; Chiang et al., 2020). The increased rainfall in southern (especially in southwestern) and northeastern China then leads to the observed negative shifts in stalagmite δ^{18} O. On the other hand, Xinglong Cave is located at the northern margin of the ASM. Apart from the effect of monsoonal precipitation, the rapid transmission of northern high-latitude climate signals could also exacerbate rapid shifts in its $\delta^{18}O$ at the onset of the last interglacial (Duan et al., 2019). Although the northern edge of the ASM also receives abundant monsoonal precipitation, the northward positioning of the westerly jet could induce a blocking effect, i.e., it could impede the transfer of ¹⁸Odepleted monsoonal moisture from the low to the mid-to highlatitudes (Nagashima et al., 2011; Chiang et al., 2015; Jia et al., 2022a; Liu et al., 2022). Since both Wanxiang Cave and

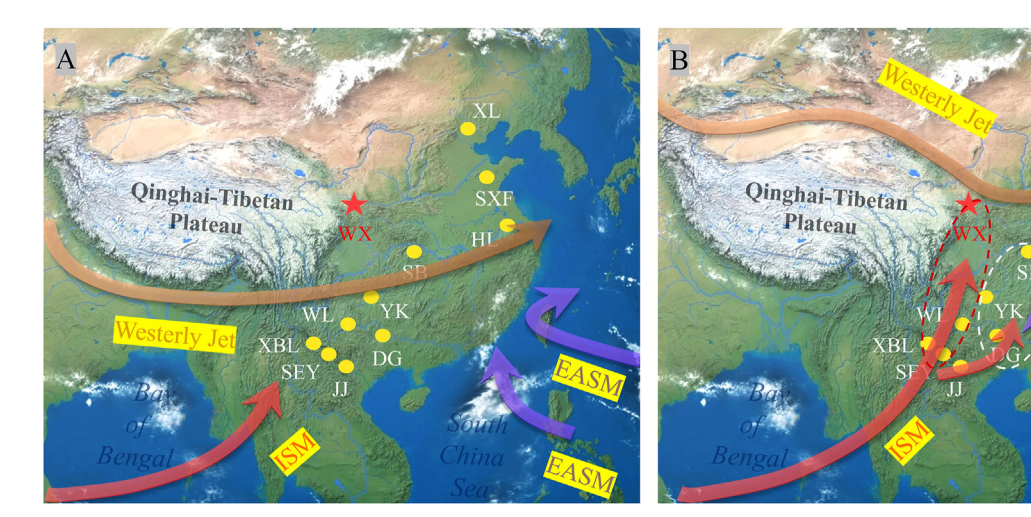


Fig. 5. Scheme showing the mechanisms explaining the differences between Chinese stalagmite δ^{18} O during HS 11 (A) and at the onset of the last interglacial (B). Enhanced ISM (red arrows) carried distal moisture and water vapor from the tropical Indian Ocean to southwestern and western China, influencing the δ^{18} O records of the WL, SEY, XBL, JJ, and WX caves (red dashed circle; 'Group 1' mentioned in Fig. 3). Both the ISM and EASM (purple arrows) may have regulated the hydroclimate in southern China, including the DG, YK, and SB caves (white dashed circle; 'Group 2' referenced in Fig. 3). Northern (XL and SXF caves) and eastern (HL cave) China were mainly controlled by the strengthened EASM (yellow dashed circle; 'Group 3' indicated in Fig. 3), which carried proximal moisture and water vapor from the western North Pacific and the South China Sea. During the HS 11 period, the westerly jet (dark yellow arrow) was relatively stronger than the ASM and was located at the south of the Qinghai-Tibetan Plateau under the severe cold condition (Nagashima et al., 2007, 2011), which prevented the moisture and water vapor from penetrating inland (Zhang et al., 2018; Li et al., 2019; Chiang et al., 2020); At the onset of the last interglacial, the westerly jet jumped abruptly to the north of the Qinghai-Tibetan Plateau and influenced the stalagmite δ¹⁸O in latitudinal direction (WX, SXF) via the blocking effect, and also allowed the moisture and water vapor carried by monsoon to intrude inland (Chiang et al., 2015; He et al., 2021). The marked locations of the westerly jet refer to Nagashima et al. (2011).

Shangxiaofeng Cave are under the influence of the more northward-positioned westerly jet (Fig. 5B), the blocking effect of the jet prevented moisture with more negative δ^{18} O from reaching the two caves but still promote local precipitation increase (e.g., Nagashima et al., 2011; Chiang et al., 2015; He et al., 2021). Hence, their stalagmite δ^{18} O records show a relatively gradual negative shift at the onset of the last interglacial (Fig. 3A and J). Due to the rapidly northward migration of the westerly jet relative to the Oinghai-Tibetan Plateau, the EASM rainband moved to the north earlier and carries precipitation with less negative δ^{18} O from the South China Sea and/or the western North Pacific to the northwestern ASM margin (Nagashima et al., 2013; Kong et al., 2017; Chiang et al., 2020). More ¹⁸O-enriched precipitation falling at Wanxiang Cave relative to ¹⁸O-depleted water vapor from the distal Indian Ocean could obscure the abrupt decrease in δ^{18} O (Jia et al., 2022a). Located close to the western North Pacific, Shangxiaofeng Cave is also affected by the EASM (Fig. 5B) (Xue et al., 2019). Accordingly, due to the proximal moisture source, the amplitude variations of its δ^{18} O record are not larger relative to Wanxiang Cave, which is on another hand mainly regulated by the ISM with the distal moisture source, resulting in a wide range of its δ^{18} O record (Jia et al., 2022a). Apart from the role of the westerly jet, seasonal moisture recycling (Baker et al., 2015) and local evaporation (Duan et al., 2016) have a larger effect on δ^{18} O at Wanxiang site than in southern China, and they may have also contributed to the gradual shift of WXZ05-12 δ^{18} O records during the glacialinterglacial transition (Jia et al., 2022a).

4.3. The 'YD-like' event during the penultimate deglaciation

The YD cold event is a unique feature of the last deglaciation when compared to previous deglaciations (Carlson, 2008). Some paleoclimate records show a cold event similar to the YD after the last interglacial onset, i.e., a YD-like event, resulting in a two-step deglaciation (Seidenkrantz et al., 1996; Sima et al., 2004; Regattieri et al., 2014). This YD-like event is also recorded by an

abrupt positive δ^{18} O shift (~3.0%) at ~128.5 kyr B.P. in Shangxiaofeng Cave record from northern China (Fig. 6B) (Xue et al., 2019). However, other Chinese stalagmite records do not exhibit a positive δ^{18} O excursion during the same time period (Fig. 6). Although stalagmite WXZ05-12 records a centennial-scale increase in δ^{18} O at ~129.7 kyr B.P., its amplitude (~0.9%) is much smaller than that (~3.0%) in Shangxiaofeng Cave (Fig. 6B). Hence, the YDlike event, at least, did not have far-reaching impacts on the CMR. On the other hand, WXZ05-12 δ^{18} O reveals a persistent oscillation from 128.9 to 128.5 kyr B.P. on centennial timescales (Fig. 6A). According to Duan et al. (2019), there was a 'pause' event in northern China (Fig. 6C) (i.e., minimal $\,\delta^{18}O$ shift) following the onset of the last interglacial, while a 'slowdown' pattern in southern China (i.e., negative δ^{18} O shift but with a smaller slope) (Fig. 6G-K). The relatively lower resolution of Hulu, Yangkou, and Xiaobailong Cave δ^{18} O records (Fig. 6D–F), however, makes it difficult to determine the occurrence of a 'slowdown' pattern in these records. But by this definition, our oscillated δ^{18} O variations well correspond to the 'pause' event in northern China within their chronological uncertainties, implying a common climate change pattern in both western and northern China after the onset of the last interglacial, but in contrast to southern China. Therefore, the YD-like event during the penultimate deglaciation may not be as prominent as it was during the last deglaciation. In other words, the YD-like event probably did not lead to cold and severe climate conditions across the CMR (Kelly et al., 2006; Carlson, 2008; Bauch et al., 2012; Marino et al., 2015; Duan et al., 2019). The occurrence of a YD-like event requires a strong IRD event with an obvious decrease in AMOC intensity analogous to that of the YD during Termination I. A new high-resolution AMOC record does not show a second significant AMOC shutdown in the North Atlantic during the penultimate deglaciation (Fig. 4B; Deaney et al., 2017). The intensity of the IRD event was also weak and even did not occur (Fig. 4A; Oppo et al., 2006; Mokeddem et al., 2014; Marino et al., 2015). Indeed, the rapid retreat of Northern Hemisphere ice sheets under a strengthened NHSI prevented the AMOC from reaching to a

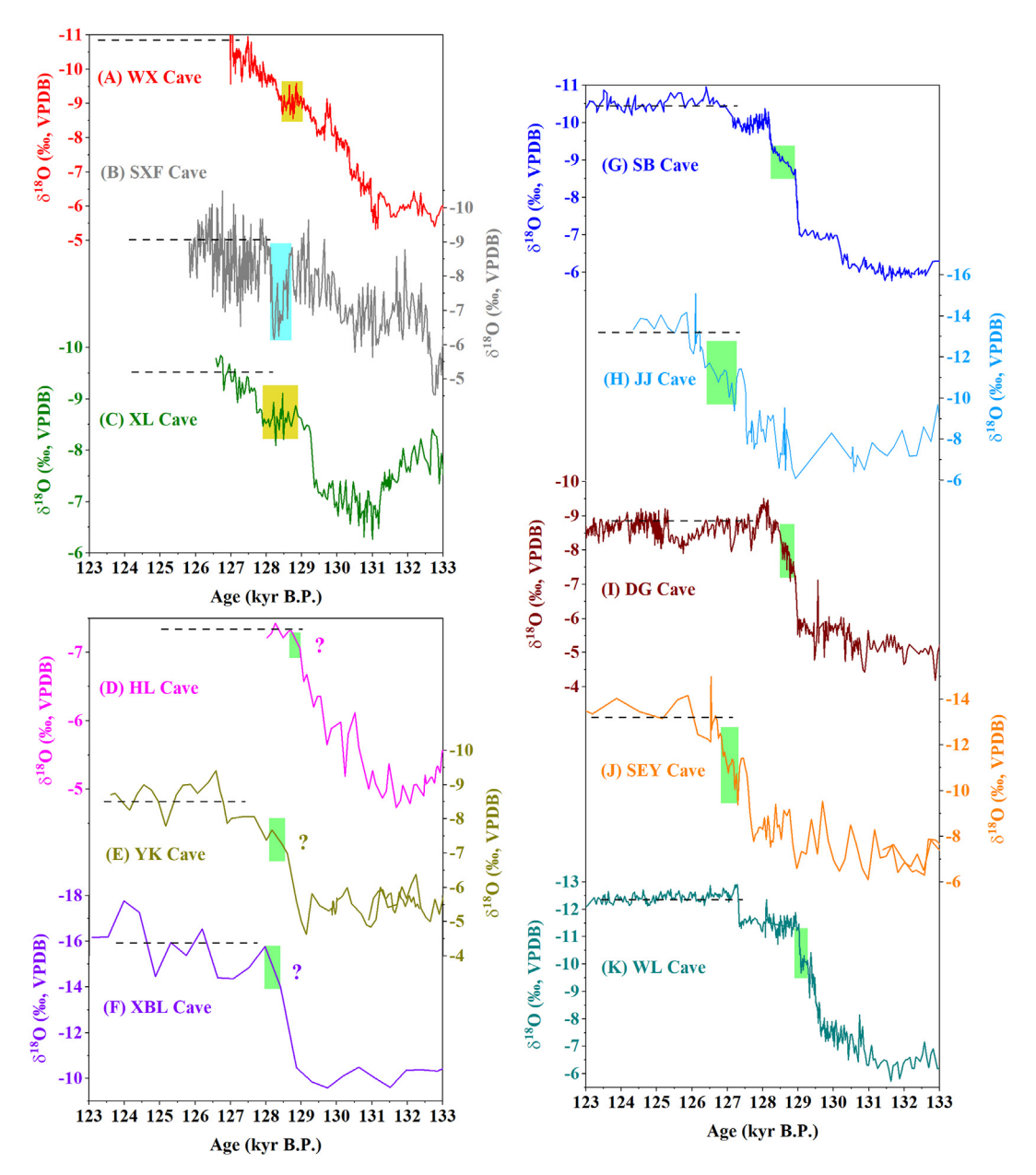


Fig. 6. A comparison of Chinese stalagmite δ^{18} O records between 133 and 123 kyr B.P. (A) Wanxiang Cave (WX; this study); (B) Shangxiaofeng Cave (SXF; Xue et al., 2019); (C) Xinglong Cave (XL; Duan et al., 2019); (D) Hulu Cave (HL; Cheng et al., 2006); (E) Yangkou Cave (YK; Li et al., 2014); (F) Xiaobailong Cave (XBL; Cai et al., 2015); (G) Sanbao Cave (SB; Cheng et al., 2009); (H) Jiangjun Cave (JJ; Wassenburg et al., 2021); (I) Dongge Cave (DG; Kelly et al., 2006); (J) Southeast Yunnan Cave (SEY; Liu et al., 2020); (K) Wulu Cave (WL; Li et al., 2022). The green and dark yellow bars represent the climate 'slowdown' avenus after the onset of the last interglacial, respectively (Duan et al., 2019). It is still uncertain whether there is a 'slowdown' pattern in the Hulu, Yangkou, and Xiaobailong Cave δ^{18} O records because of their relatively lower resolution (Cheng et al., 2006; Li et al., 2014; Cai et al., 2015). The blue bar marks a YD-like event identified by Xue et al. (2019). The black lines indicate the end of the last interglacial period.

completely vigorous state after Termination II (129–130 kyr B.P.), and thus the additional flux of freshwater into the North Atlantic induced a weaker effect on the AMOC than its counterpart during Termination I (Carlson, 2008; Masson-Delmotte et al., 2010; Govin et al., 2012; Marino et al., 2015; Deaney et al., 2017; Gorbarenko et al., 2019; Stoll et al., 2022). Despite its abrupt strengthening at ~129 kyr B.P., the NADW did not completely recover until ~127.5 kyr B.P. (Fig. 4C; Böhm et al., 2015). This suggests a continuous increase in northward moisture and heat transport even after the onset of the last interglacial. A study on two marine sediments cores from the North Atlantic (Bauch et al., 2012) further points to the apparent lack of the YD-like event, possibly due to rapid environmental and global sea level changes. In summary, the specific

Chinese stalagmite δ^{18} O change after the onset of the last interglacial is regarded as a short period of decreased ASM corresponding to a mild cold event caused by a slightly weakened AMOC, but not a YD-like event (Duan et al., 2019; Stoll et al., 2022; Weldeab et al., 2022).

4.4. Change in $\delta^{18}\text{O}$ amplitude from the late penultimate glacial to the last interglacial

Noteworthy disparities among Chinese stalagmite δ^{18} O records also exist, in particular, during the period from the late penultimate glacial to the last interglacial. We determined δ^{18} O amplitude for each site, i.e., the difference between δ^{18} O of the last interglacial

period and that of the period with an abrupt δ^{18} O shift right before HS 11 (Fig. 3) (Xue et al., 2019). The results reveal a decrease in the amplitude of stalagmite δ^{18} O from southwestern to northeastern China. The largest amplitude is observed in Southeast Yunnan Cave (~4.5%), Wulu Cave (~4.6%), Jiangjun Cave (~4.1%), and Xiaobailong Cave (~4.7%) (Fig. 3B-E), all caves located in southwestern China. The amplitude recorded by the Yangkou Cave. Dongge Cave. and Sanbao Cave records from South Central China is ~1.6%. ~2.2%. and ~2.4‰, respectively (Fig. 3F–H). δ^{18} O of Hulu (eastern China) and Shangxiaofeng (northern China) caves exhibits a much smaller amplitude, i.e., ~0.6% and ~0.7%, respectively (Fig. 3I–J). Although the Xinglong Cave δ^{18} O record (northeastern China) does not cover the pre-HS 11 period, its δ^{18} O amplitude is probably lower than ~1.2%, given the lowest δ^{18} O during HS 11, and thus its amplitude is comparable to that of the Hulu and Shangxiaofeng δ^{18} O records (Fig. 3K) (Duan et al., 2019). The altitude of cave sites might be a possible reason for this difference (Cai et al., 2012), such as that the higher the altitude, the larger the amplitude of δ^{18} O variations. However, for example, Yangkou Cave at a higher altitude (~2140 m) records a smaller amplitude (~1.6%) (Fig. 3F) while Jiangjun Cave at a lower altitude (200 m) exhibits a larger amplitude (~4.1%) (Fig. 3D). Therefore, the cave elevation cannot be a main cause of the spatial pattern of δ^{18} O amplitude changes.

Another possible cause is the distance between the cave sites and moisture sources in tropical oceans. Precipitation $\delta^{18}O$ decreases along the distance from the ocean to the cave sites, which might mute the contrast of precipitation $\delta^{18}O$ when the coast retreats from a glacial period to an interglacial period (Xue et al., 2019). However, both Xiaobailong and Dongge caves are located close to the South China Sea (Fig. 1), but their $\delta^{18}O$ records show quite different amplitudes; ~4.7% in Xiaobailong Cave and only ~2.2% in Dongge Cave. Moreover, although being far away from the ocean, Wanxiang Cave has a lager amplitude in $\delta^{18}O$ (~5.2%) relative to southern caves (Fig. 3A). Accordingly, the distance change between caves and oceanic moisture sources due to sea level fluctuations should also have a limited effect to the $\delta^{18}O$ differences.

The transport pathway effect has been proposed to account for the glacial-interglacial variability in Chinese stalagmite δ^{18} O records (Liu et al., 2020); an increase in rainfall amount with weaker isotope fractionation along the moisture pathway results in a lower amplitude variation in δ^{18} O record from glacial to interglacial periods. This hypothesis seems to explain the decreasing amplitudes of δ^{18} O change from southwestern to northeastern China. However, it requires a single moisture source along the moisture transport pathway, that is, the pathway from the southwestern China. But the moisture for sites in northern and eastern China, such as Xinglong Cave, Shangxiaofeng Cave, and Hulu Cave, mainly comes from the western Pacific (Cheng et al., 2006; Duan et al., 2019; Xue et al., 2019). The transport pathway effect thus should have less influence on stalagmite δ^{18} O at these sites. The moisture sourced from the tropical western Pacific and South China Sea contributes more to the δ^{18} O variation in the north and east CMR. In contrast, Wanxiang, Wulu, Xiaobailong, Jiangjun, and Southeast Yunnan caves are dominantly influenced by the ISM (Cai et al., 2015; Liu et al., 2020, 2022; Wassenburg et al., 2021; Jia et al., 2022a). The ISM carries more water vapor with lower δ^{18} O values from the distal tropical Indian Ocean to southwestern and western China, resulting in significantly negative $\delta^{18}\text{O}$ values and a large amplitude change in the speleothem records (Fig. 5B) (Jia et al., 2022a). On the other hand, Dongge, Yangkou, and Sanbao caves may largely have been under the influence of both the ISM and EASM (Maher, 2008). The EASM brings rainfall with relatively higher δ^{18} O to the regions adjacent to the South China Sea and/or western Pacific (Clemens et al., 2010; Tan, 2014). As a result, stalagmite records from these

three caves show relatively moderate δ^{18} O changes. We note that. however, there is insufficient data to quantify the relative contributions of these two pathways. Situated close to the tropical western Pacific, Shangxiaofeng, Xinglong, and Hulu caves are controlled by the EASM and thus receive a large amount of precipitation with higher δ^{18} O (Cheng et al., 2006; Duan et al., 2019; Xue et al., 2019). When located at the north of the Oinghai-Tibet Plateau, the westerly jet likely blocked the negative shifts in Wanxiang Cave $\delta^{18}\text{O}$, but it only mitigated the abrupt shift in $\delta^{18}\text{O}$ at the onset of the last interglacial without impact on the overall δ^{18} O amplitude during Termination II. Continuously increasing ISM intensity carried more ¹⁸O-depeleted precipitation to Wanxiang Cave during the last interglacial period, resulting in more negative δ^{18} O and thus a large amplitude in the record (Jia et al., 2022a). Overall, the differences in the Chinese stalagmite $\delta^{18}O$ change from the late penultimate glacial to the last interglacial are most likely regulated by their moisture sources (Cai et al., 2015). Simply, the ISM and EASM can leave different hydroclimatic imprints at different geographic locations of the CMR (Wassenburg et al., 2021).

5. Conclusions

We represent a high-resolution δ^{18} O record of a precisely dated stalagmite spanning the period from 133.1 to 127.0 kyr B.P. from Wanxiang Cave, western China. This record primarily documents precipitation $\delta^{18}\text{O}$ changes associated with the ASM intensity on millennial to centennial timescales. Relatively higher δ^{18} O values during the WMI mimic other Chinese stalagmite δ^{18} O records, further illustrating the close teleconnection between the ASM and the North Atlantic cold event (HS 11). Our δ^{18} O exhibits a gradual decrease at the onset of the last interglacial rather than an abrupt shift reflected by other cave $\delta^{18}O$ records from the CMR. Such discrepancy is probably associated with the rapid jump of the westerly jet to the north of the Qinghai-Tibet Plateau. This northward displacement of the jet suppressed the penetration of lowlatitude ¹⁸O-depletion moisture and induced more precipitation with less negative δ^{18} O from the earlier northward EASM rain belt to Wanxiang Cave. In addition, we did not observe YD-like event in the Wanxiang δ^{18} O record. The dissimilarities among the Chinese stalagmite δ^{18} O records during the transition from the late penultimate glacial to the last interglacial were largely related to the changes in monsoonal moisture sources.

Author contributions

Wei Jia prepared the manuscript and figures; Wei Jia, Pingzhong Zhang, Xianfeng Wang, and R. Lawrence Edwards conceived the project and structure; Binggui Cai was responsible for stable isotopic analyses and Hai Cheng, Youfeng Ning, and R. Lawrence Edwards for ²³⁰Th dating; Pingzhong Zhang, Xianfeng Wang, Shaoneng He, Guangxin Liu, Shufang Yuan, and Qibin Sun contributed to the manuscript revision at different stages; Hongyu Shi, Wenfei Zhang, Ruitao Deng, Tao Gao, Leilei Zhang performed the field work and prepared the isotope data; Pingzhong Zhang, Xianfeng Wang, Shaoneng He, Hai Cheng, and R. Lawrence Edwards supervised this work. All authors contributed to the discussion of the manuscript.

Declaration of competing interest

The authors declare that they have no known competing financial interests or personal relationships that could have appeared to influence the work reported in this paper.

Data availability

We have shared the data in the attached file

Acknowledgments

We greatly appreciate the constructive comments of the editor Dr. Miryam Bar-Matthews and the three anonymous reviewers. Special thanks go to Prof. Haiwei Zhang for his comments on our paper. This work was supported by grants of the National Natural Science Foundation of China (No. 41873001, 41473009, 41273014, 42101024), China Scholarship Council (No. 202006180039), Department of Earth and Environmental Sciences, University of Minnesota, USA (U.S. NSF Grant 2202913 to R.L.E), and Isotope Laboratory of Xi'an Jiaotong University, China. X.F.W. acknowledges the financial support by the Ministry of Education, Singapore through an MOE Tier 2 grant (MOE2019-T2-1-174) and the Earth Observatory of Singapore (EOS). This work comprises EOS contribution number 502.

Appendix A. Supplementary data

Supplementary data to this article can be found online at https://doi.org/10.1016/j.quascirev.2023.108193.

References

- Baker, A.J., Sodemann, H., Baldini, J.U.L., Breitenbach, S.F.M., Johnson, K.R., van-Hunen, J., Zhang, P.Z., 2015. Seasonality of westerly moisture transport in the East Asian summer monsoon and its implications for interpreting precipitation δ¹⁸O. J. Geophys. Res. 120 (12), 5850–5862.
- Bauch, H.A., Kandiano, E.S., Helmke, J.P., 2012. Contrasting ocean changes between the subpolar and polar North Atlantic during the past 135 ka. Geophys. Res. Lett. 39. 1.11604.
- Berger, A., 1978. Long-term variations of caloric insolation resulting from the earth's orbital elements. Quat. Res. 9 (2), 139–167.
- Böhm, E., Lippold, J., Gutjahr, M., Frank, M., Blaser, P., Antz, B., Fohlmeister, J., Frank, N., Andersen, M.B., Deininger, M., 2015. Strong and deep Atlantic meridional overturning circulation during the last glacial cycle. Nature 517 (7532), 73–76.
- Cai, Y.J., Zhang, H.W., Cheng, H., An, Z.S., Edwards, R.L., Wang, X.F., Tan, L.C., Liang, F.Y., Wang, J., Kelly, M.J., 2012. The Holocene Indian monsoon variability over the southern Tibetan Plateau and its teleconnections. Earth Planet Sci. Lett. 335–336, 135–144.
- Cai, Y.J., Fung, I.Y., Edwards, R.L., An, Z.S., Cheng, H., Lee, J.E., Tan, L.C., Shen, C.C., Wang, X.F., Day, J.A., Zhou, W.J., Kelly, M.J., Chiang, J.C.H., 2015. Variability of stalagmite-inferred Indian monsoon precipitation over the past 252,000 y. Proc. Natl. Acad. Sci. USA 112 (10), 2954–2959.
- Cai, Z.Y., Tian, L.D., Bowen, G.J., 2017. ENSO variability reflected in precipitation oxygen isotopes across the Asian Summer Monsoon region. Earth Planet Sci. Lett. 475, 25–33.
- Carlson, A.E., 2008. Why there was not a younger dryas-like event during the penultimate deglaciation. Quat. Sci. Rev. 27, 882–887.
- Cheng, H., Edwards, R.L., Wang, Y.J., Kong, X.G., Ming, Y.F., Kelly, M.J., Wang, X.F., Gallup, C.D., Liu, W.G., 2006. A penultimate glacial monsoon record from Hulu Cave and two-phase glacial terminations. Geology 34 (3), 217–220.
- Cheng, H., Edwards, R.L., Broecker, W.S., Denton, G.H., Kong, X.G., Wang, Y.J., Zhang, R., Wang, X.F., 2009. Ice age terminations. Science 326 (5950), 248–252.
- Cheng, H., Edwards, R.L., Shen, C.C., Polyak, V.J., Asmerom, Y., Woodhead, J., Hellstrom, J., Wang, Y.J., Kong, X.G., Spötl, C., Wang, X.F., Calvin-Alexander Jr., E., 2013. Improvements in ²³⁰Th dating, ²³⁰Th and ²³⁴U half-life values, and U-Th isotopic measurements by multi-collector inductively coupled plasma mass spectrometry. Earth Planet Sci. Lett. 371–372, 82–91.
- Cheng, H., Zhang, H.W., Zhao, J.Y., Li, H.Y., Ning, Y.F., Kathayat, G., 2019. Chinese stalagmite paleoclimate researches: a review and perspective. Sci. China Earth Sci. 62 (10), 1489–1513.
- Chiang, J.C.H., Fung, I.Y., Wu, C.-H., Cai, Y.J., Edman, J.P., Liu, Y.W., Day, J.A., Bhattacharya, T., Mondal, Y., Labrousse, C.A., 2015. Role of seasonal transitions and westerly jets in East Asian paleoclimate. Quat. Sci. Rev. 108, 111–129.
- Chiang, J.C.H., Swenson, L.M., Kong, W.W., 2017. Role of seasonal transitions and the westerlies in the interannual variability of the East Asian summer monsoon precipitation. Geophys. Res. Lett. 44 (8), 3788–3795.
- Chiang, J.C.H., Herman, M.J., Yoshimura, K., Fung, I.Y., 2020. Enriched East Asian oxygen isotope of precipitation indicates reduced summer seasonality in regional climate and westerlies. Proc. Natl. Acad. Sci. USA 117 (26), 14745–14750.

- Clemens, S.C., Prell, W.L., Sun, Y.B., 2010. Orbital-scale timing and mechanisms driving Late Pleistocene Indo-Asian summer monsoons: reinterpreting cave speleothem δ^{18} O. Paleoceanography 25 (4), PA4207.
- Deaney, E.L., Barker, S., van de Flierdt, T., 2017. Timing and nature of AMOC recovery across Termination 2 and magnitude of deglacial CO₂ change. Nat. Commun. 8 (1), 14595.
- Denton, G.H., Anderson, R.F., Toggweiler, J.R., Edwards, R.L., Schaefer, J.M., Putnam, A.E., 2010. The last glacial termination. Science 328 (5986), 1652–1656.
- Domínguez-Villar, D., Vázquez-Navarro, J.A., Krklec, K., Lojen, S., López-Sáez, J.A., Dorado-Valiño, M., Fairchild, I.J., 2020. Millennial climate oscillations controlled the structure and evolution of Termination II. Sci. Rep. 10 (1), 14912.
- Dorale, J.A., Liu, Z., 2009. Limitations of Hendy test criteria in judging the paleoclimatic suitability of speleothems and the need for replication. J. Cave Karst Stud. 71 (1), 73–80.
- Drysdale, R.N., Hellstrom, J.C., Zanchetta, G., Fallick, A.E., Sánchez Goñi, M.F., Couchoud, I., McDonald, J., Maas, R., Lohmann, G., Isola, I., 2009. Evidence for obliquity forcing of glacial Termination II. Science 325, 1527–1531.
- Duan, W.H., Ruan, J.Y., Luo, W.J., Li, T.Y., Tian, L.J., Zeng, G.N., Zhang, D.Z., Bai, Y.J., Li, J.L., Tao, T., Zhang, P.Z., Baker, A., Tan, M., 2016. The transfer of seasonal isotopic variability between precipitation and drip water at eight caves in the monsoon regions of China. Geochem. Cosmochim. Acta 183, 250–266.
- Duan, W.H., Cheng, H., Tan, M., Li, X.L., Edwards, R.L., 2019. Timing and structure of Termination II in north China constrained by a precisely dated stalagmite record. Earth Planet Sci. Lett. 512, 1–7.
- Duan, W.H., Wang, X., Tan, M., Cui, L.L., Wang, X.F., Xiao, Z.Y., 2022. Variable phase relationship between monsoon and temperature in East Asia during Termination II revealed by oxygen and clumped isotopes of a northern Chinese stalagmite. Geophys. Res. Lett. 49 (15), e2022GL098296.

 Edwards, R.L., Chen, J.H., Wasserburg, G.J., 1987. ²³⁸U-²³⁴U-²³⁰Th-²³²Th systematics
- Edwards, R.L., Chen, J.H., Wasserburg, G.J., 1987. ²³⁸U-²³⁴U-²³⁰Th-²³²Th systematics and the precise measurement of time over the past 500000 years. Earth Planet Sci. Lett. 81 (2–3), 175–192.
- Gao, T., Zhang, P.Z., Cheng, H., Zhang, L.L., Li, X.H., Shi, H.Y., Jia, W., Ning, Y.F., Li, H.Y., Edwards, R.L., 2023. An annually laminated stalagmite from the eastern Qinghai-Tibetan Plateau provides evidence of climate instability during the early MIS 5e in the Asian summer monsoon. Sci. China Earth Sci. 66, 1147–1164.
- Gibson, K.A., Peterson, L.C., 2014. A 0.6-million-year record of millennial-scale climate variability in the tropics. Geophys. Res. Lett. 41 (3), 969–975. Gorbarenko, S.A., Malakhova, G.Y., Artemova, A.V., Bosin, A.A., Yanchenko, E.A.,
- Gorbarenko, S.A., Malakhova, G.Y., Artemova, A.V., Bosin, A.A., Yanchenko, E.A., Vasilenko, Y., 2019. Millennial scale cycles in the Bering Sea during penultimate and last glacials; their similarities and differences. Quat. Int. 525, 151–158.
- Govin, A., Braconnot, P., Capron, E., Cortijo, E., Duplessy, J.C., Jansen, E., Labeyrie, L., Landais, A., Marti, O., Michel, E., Mosquet, E., Risebrobakken, B., Swingedouw, D., Waelbroeck, C., 2012. Persistent influence of ice sheet melting on high northern latitude climate during the early Last Interglacial. Clim. Past 8 (2), 483–507.
- Grant, K.M., Rohling, E.J., Bar-Matthews, M., Ayalon, A., Medina-Elizalde, M., Bronk Ramsey, C., Satow, C., Roberts, A.P., 2012. Rapid coupling between ice volume and polar temperature over the past 150000 years. Nature 491, 744–747.
- He, C., Liu, Z.Y., Otto-Bliesner, B.L., Brady, E.C., Zhu, C., Tomas, R., Clark, P.U., Zhu, J., Jahn, A., Gu, S., Zhang, J., Nusbaumer, J., Noone, D., Cheng, H., Wang, Y., Yan, M., Bao, Y., 2021. Hydroclimate footprint of pan-Asian monsoon water isotope during the last deglaciation. Sci. Adv. 7 (4), eabe2611.
- Hendy, C.H., 1971. The isotopic geochemistry of speleothems-I. The calculation of the effects of different modes of formation on the isotopic composition of speleothems and their applicability as palaeoclimatic indicators. Geochem. Cosmochim. Acta 35 (8), 801–824.
- Hu, J., Emile-Geay, J., Tabor, C., Nusbaumer, J., Partin, J., 2019. Deciphering oxygen isotope records from Chinese speleothems with an isotope-enabled climate model. Paleoceanogr. Paleoclimatol. 34 (12), 2098–2112.
- Jia, W., Zhang, P.Z., Wang, X.F., Cheng, H., He, S.N., Shi, H.Y., Gao, T., Li, X.H., Zhang, L.L., Zhang, H.W., Li, H.Y., Edwards, R.L., 2022a. Chinese Interstadials 14-17 recorded in a precisely U-Th dated stalagmite from the northern edge of the Asian summer monsoon during the MIS 4/3 boundary. Palaeogeogr. Palaeoclimatol. Palaeoecol. 607 (3), 111265.
- Jia, W., Zhang, P.Z., Zhang, L.L., Li, X.H., Gao, T., Wang, H.C., Zhang, H.W., Li, H.Y., Cheng, H., Edwards, R.L., 2022b. Highly resolved δ¹³C and trace element ratios of precisely dated stalagmite from northwestern China: hydroclimate reconstruction during the last two millennia. Quat. Sci. Rev. 291 (7), 107473.
- Johnson, K.R., Ingram, B.L., Sharp, W.D., Zhang, P.Z., 2006. East asian summer monsoon variability during marine isotope stage 5 based on speleothem δ¹⁸O records from Wanxiang cave, central China. Palaeogeogr. Palaeoclimatol. Palaeoecol. 236 (1–2), 5–19.
- Jouzel, J., Masson-Delmotte, V., Cattani, O., Dreyfus, G., Falourd, S., Hoffmann, G., Minster, B., Nouet, J., Barnola, J.M., Chappellaz, J., Fischer, H., Gallet, J.C., Johnsen, S., Leuenberger, M., Loulergue, L., Luethi, D., Oerter, H., Parrenin, F., Raisbeck, G., Raynaud, D., Schilt, A., Schwander, J., Selmo, E., Souchez, R., Spahni, R., Stauffer, B., Steffensen, J.P., Stenni, B., Stocker, T.F., Tison, J.L., Werner, M., Wolff, E.W., 2007. Orbital and millennial Antarctic climate variability over the past 800,000 years. Science 317 (5839), 793–796.
- Kelly, M.J., Edwards, R.L., Cheng, H., Yuan, D.X., Cai, Y.J., Zhang, M.L., Lin, Y.S., An, Z.S., 2006. High resolution characterization of the Asian Monsoon between 146,000 and 99,000 years B.P. from Dongge Cave, China and global correlation of events surrounding Termination II. Palaeogeogr. Palaeoclimatol. Palaeoecol. 236 (1–2), 20–38
- Kim, S.T., O'Neil, J.R., 1997. Equilibrium and nonequilibrium oxygen isotope effects in

- synthetic carbonates. Geochem. Cosmochim. Acta 61 (16), 3461–3475.
- Kong, W.W., Swenson, L.M., Chiang, J.C.H., 2017. Seasonal transitions and the westerly jet in the Holocene East Asian summer monsoon. J. Clim. 30, 3343–3365.
- Lei, J., Shi, Z.G., Xie, X.N., Sha, Y.Y., Li, X.Z., Liu, X.D., An, Z.S., 2021. Seasonal variation of the westerly jet over Asia in the last glacial maximum: role of the Tibetan plateau heating. J. Clim. 34 (7), 2723–2740.
- Li, T.Y., Shen, C.C., Huang, L.J., Jiang, X.Y., Yang, X.L., Mii, H.S., Lee, S.Y., Lo, L., 2014. Stalagmite-inferred variability of the Asian summer monsoon during the penultimate glacial-interglacial period. Clim. Past 10 (3), 1211–1219.
- Li, Y., Song, Y.G., Yin, Q.Z., Han, L., Wang, Y.X., 2019. Orbital and millennial northern mid-latitude westerlies over the last glacial period. Clim. Dynam. 53, 3315–3324.
- Li, Y., Peng, S.M., Hao, L., Zhou, X.R., Li, H.Y., 2022. Interactions of the westerlies and Asian summer monsoon since the last deglaciation in the northeastern Qinghai-Tibet Plateau. Paleoceanogr. Paleoclimatol. 37 (11), e2022PA004548.
- Liu, G.X., Li, X.L., Chiang, H.W., Cheng, H., Yuan, S., Chawchai, S., He, S., Lu, Y., Aung, L.T., Maung, P.M., Tun, W.N., Oo, K.M., Wang, X.F., 2020. On the glacialinterglacial variability of the Asian monsoon in speleothem δ¹⁸O records. Sci. Adv. 6 (7), eaay8189.
- Liu, S.S., Liu, D.B., Wang, Y.J., Zou, L.Z., Gao, H., 2022. Spatio-temporal expressions of precessional-scale stalagmite δ^{18} O variations from the Asian monsoon area. Palaeogeogr. Palaeoclimatol. Palaeoecol. 585. 110720.
- Liu, Z.Y., Wen, X.Y., Brady, E.C., Otto-Bliesner, B., Yu, G., Lu, H.Y., Cheng, H., Wang, Y.J., Zheng, W.P., Ding, Y.H., Edwards, R.L., Cheng, J., Liu, W., Yang, H., 2014. Chinese cave records and the East Asia summer monsoon. Quat. Sci. Rev. 83, 115–128.
- Loulergue, L., Schilt, A., Spahni, R., Masson-Delmotte, V., Blunier, T., Lemieux, B., Barnola, J.M., Raynaud, D., Stocker, T.F., Chappellaz, J., 2008. Orbital and millennial-scale features of atmospheric CH₄ over the past 800,000 years. Nature 453 (7193), 383–386.
- Lourantou, A., Chappellaz, J., Barnola, J.M., Masson-Delmotte, V., Raynaud, D., 2010. Changes in atmospheric CO₂ and its carbon isotopic ratio during the penultimate deglaciation. Quat. Sci. Rev. 29, 1983–1992.
- Masson-Delmotte, V., Stenni, B., Blunier, T., Cattani, O., Chappellaz, J., Cheng, H., Dreyfus, G., Edwards, R.L., Falourd, S., Govin, A., Kawamura, K., Johnsen, S.J., Jouzel, J., Landais, A., Lemieux-Dudon, B., Lourantou, A., Marshall, G., Minster, B., Mudelsee, M., Pol, K., Röthlisberger, R., Selmo, E., Waelbroeck, C., 2010. Abrupt change of Antarctic moisture origin at the end of Termination II. Proc. Natl. Acad. Sci. USA 107 (27), 12091–12094.
- Magiera, M., Lechleitner, F.A., Erhardt, A.M., Hartland, A., Kwiecien, O., Cheng, H., Bradbury, H.J., Turchyn, A.V., Riechelmann, S., Edwards, R.L., Breitenbach, S.F.M., 2019. Local and regional Indian summer monsoon precipitation dynamics during Termination II and the last interglacial. Geophys. Res. Lett. 46 (21), 12454—12463.
- Maher, B.A., 2008. Holocene variability of the East Asian summer monsoon from Chinese cave records: a re-assessment. Holocene 18 (6), 861–866.
- Marino, G., Rohling, E.J., Rodríguez-Sanz, L., Grant, K.M., Heslop, D., Roberts, A.P., Stanford, J.D., Yu, J., 2015. Bipolar seesaw control on last interglacial sea level. Nature 522 (7555), 197–201.
- McCrea, J.M., 1950. On the isotopic chemistry of carbonates and a paleotemperature scale. J. Chem. Phys. 18, 849–857.
- Mokeddem, Z., McManus, J.F., Oppo, D.W., 2014. Oceanographic dynamics and the end of the last interglacial in the subpolar North Atlantic. Proc. Natl. Acad. Sci. USA 111 (31), 11263–11268.
- Moseley, G.E., Spötl, C., Cheng, H., Boch, R., Min, A., Edwards, R.L., 2015. Termination-II interstadial/stadial climate change recorded in two stalagmites from the north European Alps. Quat. Sci. Rev. 127, 229–239.
- Mudelsee, M., 2000. Ramp function regression: a tool for quantifying climate transitions. Comput. Geosci. 26 (3), 293–307.
- Nagashima, K., Tada, R., Matsui, H., Irino, T., Tani, A., Toyoda, S., 2007. Orbital-millennial-scale variations in Asian dust transport path to the Japan Sea. Palaeogeogr. Palaeoclimatol. Palaeoecol. 247 (1), 144–161.
- Nagashima, K., Tada, R., Tani, A., Sun, Y.B., Isozaki, Y., Toyoda, S., Hasegawa, H., 2011. Millennial-scale oscillations of the westerly jet path during the last glacial period. J. Asian Earth Sci. 40, 1214–1220.
- Nagashima, K., Tada, R., Toyoda, S., 2013. Westerly jet-East Asian summer monsoon connection during the Holocene. G-cubed 14 (12), 5041–5053.
- Oppo, D.W., McManus, J.F., Cullen, J.L., 2006. Evolution and demise of the last interglacial warmth in the subpolar North Atlantic. Quat. Sci. Rev. 25, 3268–3277.
- Orland, I.J., Edwards, R.L., Cheng, H., Kozdon, R., Cross, M., Valley, J.W., 2015. Direct measurements of deglacial monsoon strength in a Chinese stalagmite. Geology

- 43 (6), 555-558.
- Regattieri, E., Zanchetta, G., Drysdale, R.N., Isola, I., Hellstrom, J.C., Roncioni, A., 2014.
 A continuous stable isotope record from the penultimate glacial maximum to the Last Interglacial (159-121 ka) from Tana Che Urla Cave (Apuan Alps, central Italy). Quat. Res. 82, 450–461.
- Sánchez Goñi, H.M., Eynaud, F., Turon, J.L., Shackleton, N.J., 1999. High resolution palynological record off the Iberian margin: direct land-sea correlation for the Last Interglacial complex. Earth Planet Sci. Lett. 171, 123–137.
- Sato, T., 2009. Influences of subtropical jet and Tibetan Plateau on precipitation pattern in Asia: insights from regional climate modeling. Quat. Int. 194, 148–158.
- Schiemann, R., Lüthi, D., Schär, C., 2009. Seasonality and interannual variability of the westerly jet in the Tibetan Plateau region. J. Clim. 22 (11), 2940–2957. Seidenkrantz, M.S., Bornmalm, L., Johnsen, S.J., Knudsen, K.L., Kuijpers, A.,
- Seidenkrantz, M.S., Bornmalm, L., Johnsen, S.J., Knudsen, K.L., Kuijpers, A., Lauritzen, S.E., Leroy, S.A.G., Mergeai, I., Schweger, C., Vliet-Lanoë, B.V., 1996. Two-step deglaciation at the oxygen isotope stage 6/5E transition: the Zeifen-Kattegat climate oscillation. Ouat. Sci. Rev. 15 (1), 63–75.
- Kattegat climate oscillation. Quat. Sci. Rev. 15 (1), 63–75.

 Shackleton, S., Baggenstos, D., Menking, J.A., Dyonisius, M.N., Bereiter, B., Bauska, T.K., Rhodes, R.H., Brook, E.J., Petrenko, V.V., McConnell, J.R., Kellerhals, T., Häberli, M., Schmitt, J., Fischer, H., Severinghaus, J.P., 2020. Global ocean heat content in the Last Interglacial. Nat. Geosci. 13 (1), 77–81.
- Siddall, M., Bard, E., Rohling, E.J., Hemleben, C., 2006. Sea-Level reversal during termination II. Geology 34 (10), 817–820.
- Sima, A., Paul, A., Schulz, M., 2004. The Younger Dryasdan intrinsic feature of late Pleistocene climate change at millennial timescales. Earth Planet Sci. Lett. 222, 741–750.
- Skinner, L.C., Shackleton, N.J., 2006. Deconstructing terminations I and II: revisiting the glacioeustatic paradigm based on deep-water temperature estimates. Quat. Sci. Rev. 25 (23–24), 3312–3321.
- Stoll, H.M., Cacho, I., Gasson, E., Sliwinski, J., Kost, O., Moreno, A., Iglesias, M., Torner, J., Perez-Mejias, C., Haghipour, N., Cheng, H., Edwards, R.L., 2022. Rapid northern hemisphere ice sheet melting during the penultimate deglaciation. Nat. Commun. 13, 3819.
- Tan, M., 2014. Circulation effect: response of precipitation δ^{18} O to the ENSO cycle in monsoon regions of China. Clim. Dynam. 42 (3–4), 1067–1077.
- Tiwari, M., Kumar, V., Nagoji, S., Mohan, R., 2021. A 145 kyr record of upstream changes in Indian monsoon circulation and its link to southern high-latitude climate. Pol. Sci. 30, 100739.
- Tzedakis, P.C., Drysdale, R.N., Margari, V., Skinner, L.C., Menviel, L., Rhodes, R.H., Taschetto, A.S., Hodell, D.A., Crowhurst, S.J., Hellstrom, J.C., Fallick, A.E., Grimalt, J.O., McManus, J.F., Martrat, B., Mokeddem, Z., Parrenin, F., Regattier, E., Roe, K., Zanchetta, G., 2018. Enhanced climate instability in the North atlantic and southern europe during the last interglacial. Nat. Commun. 9 (1), 4235.
- Wang, Y.J., Cheng, H., Edwards, R.L., An, Z.S., Wu, J.Y., Shen, C.C., Dorale, J.A., 2001. A high-resolution absolute-dated late Pleistocene monsoon record from Hulu Cave, China. Science 294 (5550), 2345–2348.
- Wang, Y.J., Cheng, H., Edwards, R.L., Kong, X.G., Shao, X.H., Chen, S.T., Wu, J.Y., Jiang, X.Y., Wang, X.F., An, Z.S., 2008. Millennial and orbital scale changes in the East Asian monsoon over the past 224000 years. Nature 451 (7182), 1090–1093.
- Wassenburg, J.A., Vonhof, H.B., Cheng, H., Martínez-García, A., Ebner, P.R., Li, X.L., Zhang, H.W., Sha, L.J., Tian, Y., Edwards, R.L., Fiebig, J., Haug, G.H., 2021. Penultimate deglaciation Asian monsoon response to North Atlantic circulation collapse. Nat. Geosci. 14 (12), 937–941.
- Weldeab, S., Schneider, R.R., Yu, J.M., Kylander-Clark, A., 2022. Evidence for massive methane hydrate destabilization during the penultimate interglacial warming. Proc. Natl. Acad. Sci. USA 119 (35), e2201871119.
- Xue, G., Cai, Y.J., Ma, L., Cheng, X., Cheng, H., Edwards, R.L., Li, D., Tan, L.C., 2019. A new speleothem record of the penultimate deglacial: insights into spatial variability and centennial-scale instabilities of East Asian monsoon. Quat. Sci. Rev. 210, 113–124.
- Zhang, H.B., Griffiths, M.L., Chiang, J.C.H., Kong, W.W., Wu, S.T., Atwood, A., Huang, J.H., Cheng, H., Ning, Y.F., Xie, S.C., 2018. East Asian hydroclimate modulated by the position of the westerlies during Termination I. Science 362 (6414), 580–583.
- Zhang, P.Z., Johnson, K.R., Chen, Y.M., Chen, F.H., Ingram, B., Zhang, X.L., Zhang, C.J., Wang, S.M., Pang, F.S., Long, L.D., 2004. Modern systematics and environmental significance of stable isotopic variations in Wanxiang Cave, Wudu, Gansu, China. Chin. Sci. Bull. 49, 1649–1652.
- Zhang, P.Z., Cheng, H., Edwards, R.L., Chen, F.H., Wang, Y.J., Yang, X.L., Liu, J., Tan, M., Wang, X.F., Liu, J.H., An, C.L., Dai, Z.B., Zhou, J., Zhang, D.Z., Jia, J.H., Jin, L.Y., Johnson, K.R., 2008. A test of climate, sun, and culture relationships from an 1810-Year Chinese cave record. Science 322 (5903), 940–942.